Empirical Formulas for Estimating Self and Mutual Inductances of Toroidal Field Coils and Structures

Yasuyuki ITOH, Hiroyasu UTOH[1,2], Yoshiteru SAKAMOTO[1,2],
Ryoji HIWATARI[1,2] and Joint Special Design Team for Fusion DEMO[2]

Fukui University of Technology, Fukui 910-8505, Japan
[1]*National Institutes for Quantum and Radiological Science and Technology, Rokkasho, Aomori 039-3212, Japan*
[2]*Joint Special Design Team for Fusion DEMO*

(Received 6 July 2020 / Accepted 16 September 2020)

Self and mutual inductances of toroidal-field (TF) coils are empirically expressed by linear combinations of three coil-shape parameters: elongation, aspect ratio, and triangularity, based on their calculation results with the Neumann formula. A regression function was also obtained for calculating rough values of self-inductances of toroidal-shape structures such as a vacuum vessel in a Tokamak-type fusion reactor. An analysis for their eddy currents induced during fast discharge of TF coils is presented for showing as an application example of these formulas.

Keywords: nuclear fusion, demo reactor, toroidal field coil, inductance, eddy current, fast discharge

DOI: 10.1585/pfr.15.1405078

1. Introduction

Analyses for electromagnetic dynamics of TF coils are required for estimating thermal and mechanical impacts on related reactor structures during their fast discharge in emergency conditions such as loss of superconductivity (quench) or loss of cyclic symmetry [1, 2]. The most important quantities required for these analyses are self and mutual inductances of TF coils used in their circuit equations [3].

The self inductance of TF coil set becomes larger with increasing its size as in the case of fusion demo reactors [4] that have enormous magnetic stored energy to be thermally and safely dissipated during the fast discharge [2]. These inductances are accurately and numerically evaluated by the well-known Neumann formula [5]. The Neumann formula, however, requires us to carry out many complicated line integrals along conductor-current paths distributed in 3D-space.

Estimation of eddy currents induced in toroidal-shape structures such as a vacuum vessel during the TF-coil fast discharge is also important for consideration of their structural integrity and often analyzed prior to structural analyses with a general purpose numerical calculation code such as ANSYS [6] or a dedicated code for transient electromagnetic analyses such as EDDYCAL [7]. These electromagnetic structural analyses are not easy because they need detailed 3D-modeling of structures and long computation time and therefore it would be necessary to verify and understand their results consisted of massive numerical data by preliminary simple analyses.

In the simplified analysis for eddy currents, they can be estimated by setting up circuit equations that include circuit constants for TF coils and related structures, i.e., their resistances, self and mutual inductances. These circuit constants should also be easily evaluated for convenience from dimensions given in their design drawings.

In this paper, we will present empirical formulas for evaluating self and mutual inductances of TF coils and toroidal-shape structures with defining their cross-sectional shape parameters such as elongation, aspect ratio, and triangularity. For showing an example of application of the simplified inductance calculation, we will also demonstrate an analysis of eddy currents induced in TF-coil structures and the vacuum vessel in the fast discharge of TF coils of a fusion demo reactor, JA DEMO [4], for rough estimations of their thermal and mechanical impacts.

2. Inductance of Toroidal Structure

2.1 General formula

A mutual-inductance between toroidal-shape structures would be approximated by calculating coupled toroidal magnetic flux inside their poloidal current center lines (CCL). The mutual inductance M_{ij} between the i-th and j-th structures with a volume V_i is then estimated from

$$\begin{aligned} M_{ij}I_j &\approx N_i \int_i BdS = N_i \int_i B(R)dRdZ \\ &\approx \frac{\mu_0 N_i N_j I_j}{2\pi}(H_i + H_i{}')\xi_i, \end{aligned} \tag{1}$$

with the inductance factor

$$\xi_i = \frac{1}{H_i + H_i{}'} \int_i \left(\frac{|Z(R)|}{R} + \frac{|Z'(R)|}{R} \right) dR \text{ for } V_i \subseteq V_j,$$

author's e-mail: y-itoh@fukui-ut.ac.jp

where I is the poloidal current, N the number of turns, $B \approx \mu_0 N_j I_j/(2\pi R)$ the toroidal magnetic flux density generated by j-th current, R and Z are radial and axial coordinates of a point on the CCL, respectively, H the height of CCL (maximum value of Z) and the prime (') denotes quantities below its equatorial planes (see Fig. 1).

We have $M_{ij} = M_{ji} \approx (\mu_0 N_i N_j/2\pi)(H_i + H_i')\xi_i$ from Eq. (1) and the self-inductance $L_i = M_{ii}$. The formula for calculating the inductance factor ξ_i was analytically derived based on the geometry shown in Fig. 1, which is presented in Appendix A.

2.2 Shape parameters of toroidal structure

We define the following parameters as being used for a Tokamak plasma to express the poloidal cross-sectional shape: elongation $\kappa = H/a$, aspect ratio $A = \overline{R}/a$, and triangularity $\delta = (\overline{R} - R_M)/a$, where R_M is the radius at which $Z = H$, $\overline{R} = (R_O + R_I)/2$ the major radius, $a = (R_O - R_I)/2$ the minor radius with R_I and R_O being the inboard and outboard radii, respectively, (see Fig. 1). Using the defined parameters and the height H, we inversely obtain these radii as $R_O = a(A+1)$, $R_I = a(A-1)$, $R_M = a(A-\delta)$, and $\overline{R} = aA$ with $a = H/\kappa$.

The TF coil shape (or its CCL) is usually expressed by six arcs in its design [8], as shown in Fig. 1. For a limiting case of the shape being vertically symmetric with $\theta_2 = \pi/2 - \theta_1$ and $\theta_3 = \pi/2$ in Fig. 1, radii and center coordinates of these arcs are given with parameters κ, δ, A, H, and the arc angle θ_1 as

$$R_1 = H\left(\frac{\cos\theta_1 + \iota(\sin\theta_1 - 1)}{\cos\theta_1 + \sin\theta_1 - 1}\right),$$
$$R_2 = H\left(\frac{\cos\theta_1 - 1 + \iota\sin\theta_1}{\cos\theta_1 + \sin\theta_1 - 1}\right),$$
$$R_3 = R_M - R_I = H(1-\delta)/\kappa,$$

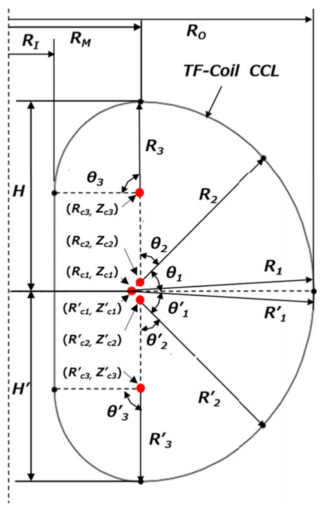

Fig. 1 Shape definition of TF-coil CCL in poloidal cross section, which is usually consisted of 6 arcs.

$$R_{c1} = R_O - R_1 = (H/\kappa)(A+1) - R_1,\ Z_{c1} = 0,$$
$$R_{c2} = R_{c1} + (R_1 - R_2)\cos\theta_1,\ Z_{c2} = (R_1 - R_2)\sin\theta_1$$
$$R_{c3} = R_{c2},\ \text{and } Z_{c3} = Z_{c2} + R_2 - R_3,$$

where $\iota = (1+\delta)/\kappa$.

Note that $\iota < 1$ and $R_1 > H$ because R_1 should be greater than R_2 and then θ_1 is inversely estimated by $2\tan^{-1}[(R_1/H - \iota)/(R_1/H - 1)] - \pi/2$ for a given radius R_1 of outboard curvature, which gives $\theta_1 \to 0$ for $R_1 \to \infty$ with $R_2 \to H_\iota = R_O - R_M$.

The cross-sectional shape of toroidal structure is thus defined by parameters κ, δ, A, and θ_1 and therefore the inductance factor ξ can be expressed as a function of them. We carried out a regression analysis with randomly generating 10^5 sets of parameters in ranges of $1.5 \le \kappa \le 2.0$, $1.5 \le A \le 2.0$, $0.22 \le \delta \le 0.5$, and $0 < \theta_1(°)/90 \le 0.7$ and obtained an empirical formula for ξ as

$$\xi = c_0 + c_\kappa\kappa + c_\delta\delta + c_{A1}A + c_{A2}A^2 + c_\theta(\theta_1/90) + \varepsilon, \quad (2)$$

with $c_0 = 4.933$, $c_\kappa = 0.03728$, $c_\delta = 0.06980$, $c_{A1} = -3.551$, $c_{A2} = 0.7629$, and $c_\theta = -0.06298$. The standard deviation of the relative error ε/ξ was then estimated to be 0.12%.

2.3 Self inductance of TF coil set

We calculated the self and mutual inductances of TF coils with the Neumann formula for the following various values of parameters: κ = 1.5, 1.6 and 1.7, δ = 0.2, 0.35 and 0.5, A = 1.5, 1.6 and 1.7, and $\theta_1(°)$ = 40, 50 and 60, all of which totally give 81 parameter combinations and CCL shape variations shown in Fig. 2 for H = 9.3 m.

In this calculation, we set geometrically imaginable current cross-sectional area (i.e. winding pack, WP) shown in Fig. 2 (b) to take its finite size into account, which would affect especially on estimations of the self-inductance

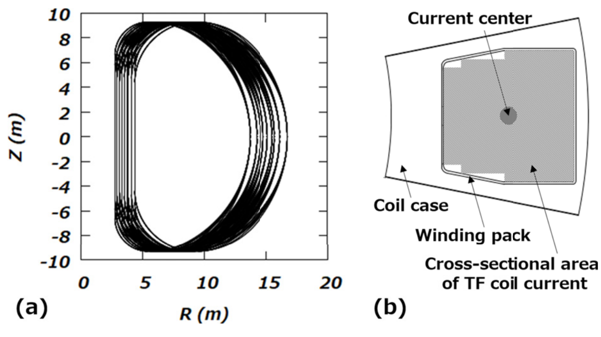

Fig. 2 Current center lines (CCL) for calculating inductances, (a) CCL shape variations for used value ranges of parameters κ, δ, A, and θ_1, (b) Inner-leg cross-sectional structure around CCL of TF coil, which is drawn only by roughly satisfying geometric constraint for each calculation case and plural conductors are distributed within the shadow region for the inductance calculation with the Neumann formula.

value of a single TF coil and the mutual one between adjacent coils. The typical sensitivity $(\delta L/L)/(\delta w/w)$ of the self inductance L of the TF-coil set was estimated for the fractional size change $(\delta w/w)$ of WP to be ~5% in the toroidal direction and 6 - 9% in the radial direction.

The self-inductance of the TF-coil set is then expressed by $L = L_O \xi_N$ with $L_O = (\mu_0/\pi)(N_{TFC} N_C)^2 H$, where ξ_N is the inductance factor given by the calculation with the Neumann formula, N_{TFC} is the number of TF coils and N_C that of turns per coil.

We first compared ξ given by Eq. (1) to ξ_N for all parameter combinations, which is shown in Fig. 3 (a). The error of ξ was then within the range of $-1.5 < (\xi - \xi_N)/\xi_N$ (%) < 0.9. Next, we assumed $\xi_N \approx \xi + \Delta\xi$ with $\Delta\xi = C_0 + C_\kappa \kappa + C_\delta \delta + C_A A$ and had optimum coefficients $C_0 = 0.05808$, $C_\kappa = -0.05846$, $C_\delta = -0.02906$, and $C_A = 0.03008$. In this case the error is reduced to $|\xi + \Delta\xi - \xi_N|/\xi_N < 0.2\%$ (see Fig. 3 (b)). Here we ignored the dependence of inductance on the arc angle θ_1 because CCL shapes are hardly changed for its value range.

We also let $\xi_N \approx \xi' = C'_0 + C'_\kappa \kappa + C'_\delta \delta + C'_A A$ without using ξ, finding optimum coefficients $C'_0 = 3.026$, $C'_\kappa = -0.03238$, $C'_\delta = 0.1091$, and $C'_A = -1.093$, which gave the error $|\xi' - \xi_N|/\xi_N < 1.4\%$ (see Fig. 3 (c)). This evaluation is the simplest method to find rough self-inductance values without calculating ξ whereas the second one (Fig. 3 (b)) gives very accurate values.

To verify these regression functions (empirical formulas), we calculated the self inductance of the ITER TF-coil set, which is reported to be 17.3 H in Ref. [2]. The ITER TF-coil CCL parameters are evaluated to be $\kappa \approx 1.57$, $\delta \approx 0.341$, $A \approx 1.68$, $\theta_1 \approx 70°$, $\theta_2 \approx 40°$, $H \approx 6.31$ m, $N_{TFC} = 18$, $N_C = 134$, and $L_O = 14.7$ H. These parameter values gave the self-inductance as $L_O \xi_N = 17.3$ H, $L_O \xi = 17.2$ H, $L_O(\xi + \Delta\xi) = 17.3$ H, and $L_O \xi' = 17.3$ H. Thus, we can immediately find the value of self inductance with the quantity L_O and three TF-coil shape parameters κ, δ, and A.

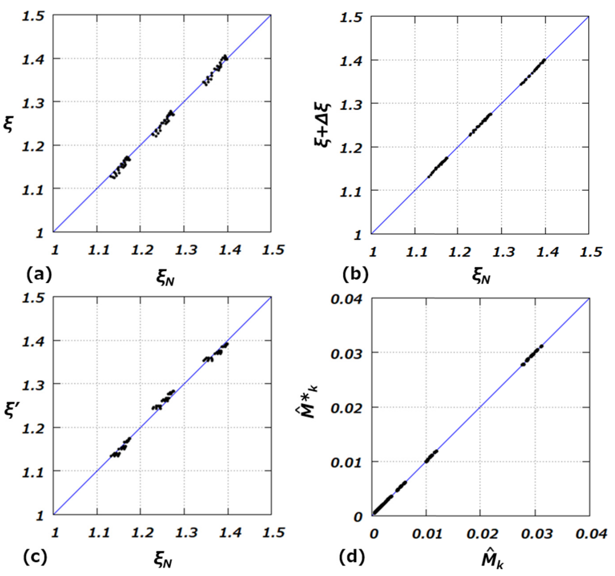

Fig. 3 Comparisons of approximated inductance factors to ξ_N and mutual inductances to $\hat{M}_k$ for all combinations of parameters, where we assume (a) $\xi_N \approx \xi$, (b) $\xi_N \approx \xi + \Delta\xi$ with $\Delta\xi = C_0 + C_\kappa \kappa + C_\delta \delta + C_A A$, (c) $\xi_N \approx \xi' = C'_0 + C'_\kappa \kappa + C'_\delta \delta + C'_A A$, and (d) $\hat{M}_k \approx \hat{M}^*_k = C''_0 + C''_\kappa \kappa + C''_\delta \delta + C''_A A$.

2.4 Mutual inductances between TF coils

Mutual inductances $M_{ij} = L_O \hat{M}_k$ with $k = |i - j|$ would also be estimated by equating

$$\hat{M}_k \approx \hat{M}^*_k = C''_{0k} + C''_{\kappa k} \kappa + C''_{\delta k} \delta + C''_{Ak} A,$$

where the normalized value $\hat{M}_k$ was found by using the Neumann formula with the number of TF-coils $N_{TFC} = 16$ selected for JA Demo design [4], i.e., $i, j = 1$ - 16, $0 \le k = |i - j| \le 8$, and $\hat{M}_{16\text{-}k} = \hat{M}_k$ for $k > 8$. Table 1 presents optimized coefficients for each k and calculated values of $\hat{M}^*_k$ are compared to $\hat{M}_k$ in Fig. 3 (d) for all cases, where the error was estimated to be $|\hat{M}^*_k - \hat{M}_k|/\hat{M}_0 < 0.7\%$, $(0 \le k \le 8)$.

Note that coefficients for $k = 0$ presented in Table 1 are not for the self inductance of TF coil set described in Sec. 2.3 but for a single TF coil.

This result, of course, is not directly applied to TF-coil designs with $N_{TFC} \neq 16$ such as the ITER TF-coil set consisted of 18 ones. Mutual inductances for $N_{TFC} = 18$ can be obtained with the following calculation procedure by assuming that $\hat{M}^*_k$ is a function of $x = k/(N_{TFC}/2)$ with $0 \le k = |i - j| \le N_{TFC}/2$, i.e., $0 \le x \le 1$.

(1) Calculate $\hat{M}^*_k$ for $k = 0, \cdots, N_{TFC}/2$ using shape parameters of concerned TF coils with $N_{TFC} = 16$.
(2) Find a regression or spline curve $f(x)$ for plots $(x_k, \hat{M}^*_k)$, where $x_k = k/(N_{TFC}/2)$ with $N_{TFC} = 16$.
(3) Calculate $\hat{M}^*_k = f(x_k)$ for $k = 0, \cdots, N_{TFC}/2$ with $N_{TFC} = 18$.

Table 1 Optimized coefficients for calculating mutual inductances of TF coils.

$k=\|i - j\|$	C''_{0k}	$C''_{\kappa k}$	$C''_{\delta k}$	C''_{Ak}
0	5.605×10^{-2}	-7.381×10^{-3}	4.258×10^{-4}	-9.303×10^{-3}
1, 15	2.355×10^{-2}	-1.792×10^{-4}	1.079×10^{-3}	-7.924×10^{-3}
2, 14	1.452×10^{-2}	4.864×10^{-4}	6.555×10^{-4}	-6.324×10^{-3}
3, 13	9.432×10^{-3}	5.613×10^{-4}	4.417×10^{-4}	-4.645×10^{-3}
4, 12	6.397×10^{-3}	5.041×10^{-4}	3.185×10^{-4}	-3.388×10^{-3}
5, 11	4.603×10^{-3}	4.307×10^{-4}	2.438×10^{-4}	-2.559×10^{-3}
6, 10	3.568×10^{-3}	3.734×10^{-4}	1.992×10^{-4}	-2.050×10^{-3}
7, 9	3.032×10^{-3}	3.383×10^{-4}	1.751×10^{-4}	-1.777×10^{-3}
8	2.866×10^{-3}	3.267×10^{-4}	1.675×10^{-4}	-1.691×10^{-3}

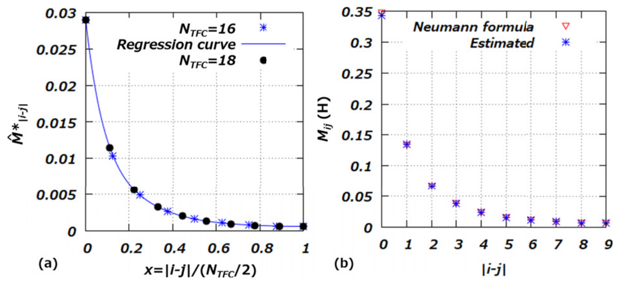

Fig. 4 Mutual inductances estimated for ITER TF coils, where (a) regression curve for plots (x_k, $\hat{M}^*{}_k$) with $N_{TFC} = 16$ and $\hat{M}^*{}_k$ calculated for $N_{TFC} = 18$ and (b) mutual inductances of ITER TF-coils estimated from this regression curve and those calculated with the Neumann formula.

(4) Calculate the normalized self-inductance $\hat{L}$ of the TF-coil set with $N' = N_{TFC}/2$

$$\hat{L} = N_{TFC}\left(\hat{M}^*{}_0 + 2(\hat{M}^*{}_1 + \cdots + \hat{M}^*{}_{N'-1}) + \hat{M}^*{}_{N'}\right).$$

(5) Calculate mutual inductances with $M_{ij} \approx \hat{M}^*{}_k L/\hat{L}$, ($k = |i - j|$), where L is the self-inductance of the TF-coil set with $N_{TFC} = 18$.

Figure 4 (a) shows the regression curve for $\hat{M}^*{}_k$ and estimated mutual inductances for ITER TF coils with $N_{TFC} = 18$, where the relative error $\varepsilon = |\hat{M}^*{}_0 - \hat{M}_0|/\hat{M}_0$ for $i = j$ was 1.4% in comparison to the value calculated with the Neumann formula (see Fig. 4 (b)). This error magnitude of M_{ii} that is the self inductance of the single TF coil is slightly higher compared to the result shown in Fig. 3 (d) with $\varepsilon < 0.7\%$.

One of this reasons would be reduction in the cross-sectional area of the TF coil current (winding pack) when N_{TFC} is increased from 16 to 18 (see Fig. 2 (b)). The size of the winding pack is decreased by ~10% in the toroidal direction and then L is increased by ~0.5% (see Sec. 2.3), which gives the increment in $\hat{M}_0$ of 1.4% as mentioned above with taking account the contribution of the self inductance $L_O\hat{M}_0$ to L being ~36%.

3. Application

Figure 5 shows an example of conceptual design drawing for JA Demo [4], which shows poloidal cross section of the TF coil and the vacuum vessel (VV). We consider poloidal eddy-current inductions in and their influences on reactor structures in the case of emergency fast discharge of the TF-coil current. Eddy currents are assumed to be induced in TF-coil structures, consisted of coil cases and radial plates (see Fig. 5), and the vacuum vessel.

Circuit equations for solving this problem are written as

$$\begin{aligned} L_1\dot{I}_1 + M_{12}\dot{I}_2 + M_{10}\dot{I}_0 + R_1I_1 &= 0 \\ L_2\dot{I}_2 + M_{21}\dot{I}_1 + M_{20}\dot{I}_0 + R_2I_2 &= 0 \end{aligned}, \qquad (3)$$

where I is the current, L the self-inductance, M the mutual inductance, R the resistance, and subscripts 0, 1, and 2 denote values of the TF-coil conductor, the coil structure, and the vacuum vessel (VV), respectively. Initial conditions are $I_1(0) = I_2(0) = 0$ and the conductor current of the TF coil is assumed to be exponentially decayed with the time constant τ_d, i.e. $I_0 = I_{OP}\exp(-t/\tau_d)$, where I_{OP} (= 83.2 kA) is the normal operating current.

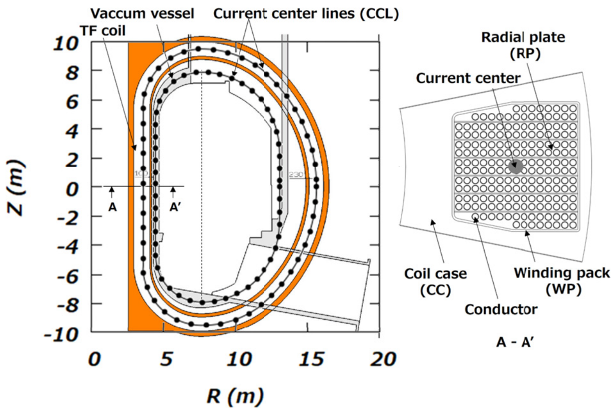

Fig. 5 Conceptual design drawing of TF coil and vacuum vessel in JA Demo, where closed line and dots denote roughly dawn poloidal current center line of each structure.

Table 2 Roughly estimated CCL-dimensions of TF coil, its structure, and vacuum vessel of JA DEMO.

	TF Coil / Structure	Vacuum Vessel
R_i (m)	3.55	4.45
R_o (m)	15.62	13.09
R_M (m)	7.66	7.88
R (m)	9.59	8.77
H (m)	9.50	7.90
a (m)	6.03	4.45
A	1.59	2.03
κ	1.58	1.83
δ	0.320	0.26
θ_1 (°)	48.0	1.0
l_{CCL} (m)	51.1	41.4

We need values of self and mutual inductances to solve the circuit equations. To find these values, we roughly drew a (almost handwritten) CCL for each structure along its contour as shown Fig. 5 (indicated by a closed line and dots), measured its dimensions, and estimated values of parameters κ, δ, A, and H, which are presented in Table 2. Note that CCL dimensions of the TF coil and its structure have nearly the same values, i.e., $H_1 \approx H_0$, $\xi_1 \approx \xi_0$ and the coil structure and the VV are regarded as single-turn coils ($N_1 = N_2 = 1$).

Self and mutual inductances of these structures are written from Eq. (1) by

$$L_0 \approx (\mu_0/\pi)N_0^2H_0\xi_0,$$

Table 3 Inductance matrix M_{ij} for reactor structures of JA DEMO shown in Fig. 5 (in H).

$i \setminus j$	0	1	2
0	4.53×10^{1}	1.47×10^{-2}	9.28×10^{-3}
1	1.47×10^{-2}	4.80×10^{-6}	3.02×10^{-6}
2	9.28×10^{-3}	3.02×10^{-6}	3.02×10^{-6}

$$L_1 \approx (\mu_0/\pi)H_1\xi_1 \approx (\mu_0/\pi)H_0\xi_0 = L_0/N_0^2,$$
$$L_2 \approx (\mu_0/\pi)H_2\xi_2,$$
$$M_{01} = M_{10} \approx (\mu_0/\pi)N_0H_0\xi_0 = L_0/N_0 = L_1N_0,$$
$$M_{02} = M_{20} \approx (\mu_0/\pi)N_0H_2\xi_2 = L_2N_0,$$
$$\text{and } M_{12} = M_{21} \approx (\mu_0/\pi)H_2\xi_2 = L_2,$$

where $N_0 = N_{TFC}N_C$ (= 16 × 192) and we assumed or approximated that coils and structures are symmetric with respect to their equatorial planes, i.e., $H_i = H_i'$. The self inductance of each structure can be evaluated by finding arc parameters R_i, θ_i, R_{ci} and Z_{ci}, (j = 1 - 3) described in Sec. 2.2 and then calculating the inductance factor ξ with the equations presented in Appendix A or the regression function Eq. (2). Table 3 presents the inductance matrix M_{ij} of the system Eq. (3).

We also need poloidal loop resistances of the TF-coil structure and the vacuum vessel. The loop resistance of the coil structure is given by $R_1 \approx \eta_{SSL}l_{CCL}/(N_{TFC}(S_{CC} + S_{RP})) \approx 1.1\,\mu\Omega$, where η_{SSL} is the resistivity of SS316 (~0.5 μΩm) at low temperature (4.2 K), l_{CCL} (≈ 51 m) the CCL length, S_{CC} (≈ 0.94 m^2) and S_{RP} (≈ 0.55 m^2) are cross-sectional area of the coil case and the radial plates, respectively.

The loop resistance of the VV was estimated from the following poloidal line integral

$$R_2 = \eta_{SSH}\oint_{VV}(2\pi R(l)\Delta(l))^{-1}dl \sim (\eta_{SSH}/\Delta_{VV})\varphi, \quad (4)$$

to be ~6.6 μΩ, where η_{SSH} is the resistivity of SS316 (0.84 μΩm) at high temperature (100°C), $\Delta(l)\sim\Delta_{VV}$ (~2 × 60 mm) the VV thickness, and a formula to calculate the factor φ (≈ 0.94) for a uniform Δ_{VV} is given in Appendix A. The conceptually designed VV is double-walled and has 20 mm-thick 64 poloidal ribs with a CCL length of ~41 m. Assuming their averaged width is roughly 1 m, we estimated their total loop resistance to be 27 μΩ that reduces the VV resistance from 6.6 μΩ to 5.3 μΩ.

Equations (3) are rewritten as

$$\dot{I}_1 + g\dot{I}_2 + \lambda_1 I_1 = \lambda_0 N_0 I_0 \text{ and } \dot{I}_1 + \dot{I}_2 + \lambda_2 I_2 = \lambda_0 N_0 I_0,$$

where

$$\lambda_0 = 1/\tau_d \ (\approx 0.033\,\mathrm{s}^{-1} \text{ for } \tau_d = 30\,\mathrm{s}),$$

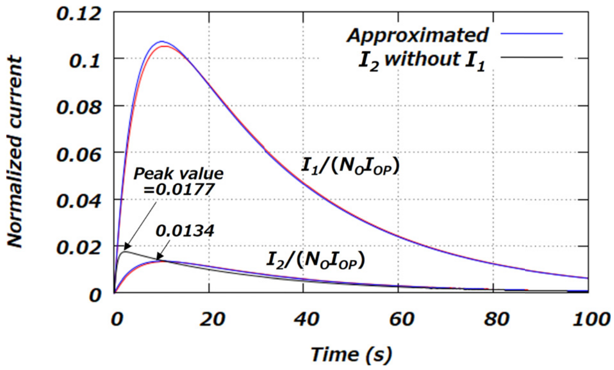

Fig. 6 Time evolutions of eddy currents induced in TF-coil structure (I_1) and vacuum vessel (I_2) (red curves) for τ_d = 30 s, where blue curves show approximated solutions for $\lambda_2 \gg \lambda_1$, λ_0, and the black curve denotes I_2 calculated by assuming I_1 = 0, i.e., there is no TF-coil structure.

$$\lambda_1 = R_1/L_1 = N_0^2R_1/L_0 \ (\approx 0.22\,\mathrm{s}^{-1}) \text{ and}$$
$$\lambda_2 = R_2/L_2 = N_0^2R_2/(gL_0) \ (\approx 1.8\,\mathrm{s}^{-1})$$

with $g = L_2/L_1$ (≈ 0.62). From these values for this case, we can say that $\lambda_2 \gg \lambda_1$, λ_0. If $I_1 \gg I_2$, the equations become

$$\dot{I}_1 + \lambda_1 I_1 = \lambda_0 N_0 I_0 \text{ and } \dot{I}_2 + \lambda_2 I_2 = \lambda_1 I_1,$$

and then we have approximated solutions

$$I_1 \approx \lambda_0 N_0 I_{OP}(e^{-\lambda_1 t} - e^{-\lambda_0 t})/(\lambda_0 - \lambda_1)$$
$$\text{and } I_2 \approx (\lambda_1/\lambda_2)I_1(\ll I_1) \text{ for } \lambda_2 \gg \lambda_1, \lambda_0.$$

Figure 6 shows time evolutions of eddy currents of the TF-coil structure (I_1) and the vacuum vessel (I_2). We see that approximated solutions are well agreed with accurate ones, i.e., the eddy current of TF-coil structure is hardly influenced by that of the VV and cannot be ignored for calculation of the latter.

The eddy current in the TF-coil structure generates Joule heat. Each conductor is heated by the Joule heat q generated in the radial plate (RP), which is estimated per unit length by

$$q = \eta_{SSL}(f_{RP}I_1/N_0)^2/(S_{RP}/N_C) \text{ with}$$
$$f_{RP} = S_{RP}/(S_{CC} + S_{RP})(\sim 0.37),$$

where f_{RP} is the area fraction of the radial plate. For the peak value of I_1 in Fig. 6, Joule heat q is estimated to be 1.8 kW/m per conductor for τ_d = 30 s and 3.3 kW/m for τ_d = 20 s, which would give no small effect on the temperature rising of the conductor in its quench event via heat conduction through a turn insulation.

The purpose of the calculation of the eddy current induced in the VV is to estimate stresses generated by the electromagnetic hoop force. The equation for roughly calculating the Tresca stress of the inboard wall is given in

Appendix B. Using this, we evaluated it for the peak current of I_2 to be 56 MPa for $\tau_d = 30$ s and 74 MPa for $\tau_d = 20$ s, which are lower than the allowable stress (∼143 MPa) of the VV material (SS316L).

The estimated Tresca stress of 56 MPa for $\tau_d = 30$ s, however, is smaller than that (∼100 MPa) obtained by a finite element analysis (FEA) [9] with nearly the same conditions. One of the reasons is that the FEA excluded the eddy current (I_1) induced in the TF-coil structure in its modeling, which increases the peak VV eddy current with a factor 1.32 (= 0.0177/0.0134, see Fig. 6), i.e., the stress estimated in the FEA should be reduced to 76 MPa. Then the relative estimation error becomes 26%. This residual error would be mainly arisen from the VV model shape drawn in Fig. 5 being quite different from the design drawing of its outboard structure that has maintenance ports.

4. Summary and Conclusions

We have presented a method for easily estimating self and mutual inductances of TF coils and toroidal-shape structures, defining their cross-sectional shape parameters.

In Chap. 2, we tried to estimate the self-inductance of TF-coil set, calculating the toroidal magnetic flux passing through the cross-sectional area enclosed by its CCL. The shape dependence of inductances is then expressed by the inductance factor ξ of a function of shape parameters: the elongation κ, the triangularity δ, the aspect ratio A, and the arc angle θ_1, and we obtained its empirical formula by a regression analysis. This formula would be useful to estimate the inductance of a toroidal-shape structure for its poloidal eddy current analysis.

The inductance factor ξ was compared to that obtained with the Neumann formula for the TF-coil set that has finite-size current-flow areas and a discontinuous structure in the toroidal direction. We found that ξ has relative errors within 1.5% in value ranges of shape parameters treated in this paper. This relative error was reduced to 0.2% by adding the correction term expressed by a linear combination of κ, δ, and A (without θ_1). The inductance value with this accuracy would be sufficient for using in the TF-coil design and its safety considerations. We also found that their linear combination directly gives the self-inductance without calculating ξ, where the relative estimation error was within 1.4% for its optimized coefficients. These empirical formulas were verified by calculating the self-inductance of the ITER TF-coil set to have its known value (= 17.3 H).

The mutual inductance M_{ij} ($1 \le i, j \le N_{TFC}/2$) was also expressed by a linear combination of κ, δ, and A with relative errors less than 0.7%. We obtained its optimum coefficients for each pair of TF coils with $N_{TFC} = 16$ and showed that this result can also be applied to the case of $N_{TFC} = 18$ selected for the ITER coil set. A bit of relative error (∼1.4%), however, appeared in the self-inductance M_{00} of a single ITER TF-coil because it becomes thinner with increasing N_{TFC}, which increases the self-inductance.

In Chap. 3 we demonstrated an analysis for eddy current inductions during the fast discharge of the TF coil set of JA DEMO, calculating self and mutual inductances of the TF-coil structure and the vacuum vessel (VV), and estimated the peak Joule heat generated in the TF-coil structure and the Tresca stress in the VV inboard wall. Although the result for the VV stress was not well agreed with the FEA due to a poor modeling of the VV structure, this simplified analysis would be useful to verify the analysis model, understand the result, and make a plan for the large scale FEA.

Acknowledgments

This work was conducted in the framework of the Joint Special Design Team for Fusion DEMO collaboration program with National Institutes for Quantum and Radiological Science and Technology, Japan.

Appendix A Inductance Factor

The inductance factor ξ in Eq. (1) is written by

$$\xi := \frac{1}{H+H'}\sum_{k=1}^{6}\int_{R_{1k}}^{R_{2k}}\frac{|Z_k(R)|}{R}dR = \sum_{k=1}^{6}\xi_k,$$

with $Z_k(R) = Z_{ck} + R_{ck}\sqrt{1-(R/R_{ck})^2}$, which becomes

$$\xi_k = \frac{1}{H+H'}\left(R_k\left|\int_{\tau_{1k}}^{\tau_{2k}}\frac{\sqrt{1-\tau^2}}{\tau+\omega_k}d\tau\right| + \left|Z_{ck}\ln\left(\frac{R_{2k}}{R_{1k}}\right)\right|\right),$$

where $\omega_k = R_{ck}/R_k$, $\tau_{sk} = (R_{sk} - R_{ck})/R_k = \cos\Theta_{sk}$, ($s = 1, 2$), with

$$\Theta_{11} = \theta_1,\ \Theta_{21} = 0,\ \Theta_{12} = \theta_1+\theta_2,\ \Theta_{22} = \theta_1,$$
$$\Theta_{13} = \theta_1+\theta_2+\theta_3 = \pi,\ \text{and}\ \Theta_{23} = \theta_1+\theta_2.$$

The integral in ξ_k is carried out analytically [10] to be

$$\begin{aligned}&\xi_k(H+H')\\ &= R_k\left|\left[\omega_k\sin^{-1}\tau + \sqrt{1-\tau^2} + p_k\Lambda(\tau,\omega_k)\right]_{\tau_{1k}}^{\tau_{2k}}\right|,\\ &\quad + \left|Z_{ck}\ln\left(\frac{R_{2k}}{R_{1k}}\right)\right| \ \text{ with } p_k = 1-\omega_k^2\end{aligned}$$

$$\text{where } \Lambda(\tau,\omega_k) = \int\frac{d\tau}{(\tau+\omega_k)\sqrt{1-\tau^2}}$$

$$= \begin{cases}\dfrac{1}{\sqrt{|p_k|}}\sin^{-1}\left(\dfrac{1+\omega_k\tau}{\tau+\omega_k}\right) & \text{for } p_k < 0\\[2ex] -\dfrac{\sqrt{1-\tau^2}}{\omega_k(\tau+\omega_k)} & \text{for } p_k = 0\\[2ex] \dfrac{1}{\sqrt{|p_k|}}\ln\left(\dfrac{2\left(1+\tau\omega_k-\sqrt{p_k(1-\tau^2)}\right)}{\tau+\omega_k}\right) & \\ & \text{for } p_k > 0.\end{cases}$$

The quantity φ in Eq. (4) that gives the VV loop resistance is also expressed by using Λ as

$$\varphi = \oint\frac{dl}{2\pi R(l)} \approx \frac{1}{2\pi}\int\sqrt{1+(dZ(R)/dR)^2}\frac{dR}{R}$$

$$= \frac{1}{2\pi}\left(\sum_{k=1}^{6}\left|\int_{\tau_{1k}}^{\tau_{2k}} \frac{d\tau}{(\tau+\omega_k)\sqrt{1-\tau^2}}\right| + \frac{Z_{c3}+|Z_{c6}|}{R_I}\right)$$
$$= \frac{\chi}{2\pi}$$

with $\chi = \dfrac{Z_{c3}+|Z_{c6}|}{R_I} + \sum_{k=1}^{6} |\Lambda(\tau_{2k},\omega_k) - \Lambda(\tau_{1k},\omega_k)|$.

Appendix B Tresca Stress in VV Wall

The Tresca stress σ_{VV} generated in the inboard wall of the vacuum vessel (VV) by its eddy current I_2 is given by $\sigma_{VV} = |\sigma_\theta - \sigma_Z|$, where σ_θ and σ_Z are principal stresses in toroidal and vertical directions, respectively. Since the toroidal magnetic field B in the VV wall is given by $B \approx B_{VVI}R_{VVI}/R$, the vertical force F_{VV} acting on the VV is estimated by

$$F_{VVZ} \approx B_{VVI}R_{VVI}I_2 \int dR/R$$
$$= B_{VVI}R_{VVI}I_2 \ln(R_{VVO}/R_{VVI}),$$

where subscripts VVI and VVO denote quantities of inboard and outboard walls of the VV, respectively. The vertical stress generated in the VV wall is then calculated by

$$\sigma_Z \approx \frac{F_{VVZ}}{2\pi\Delta_{VV}(R_{VVI}+R_{VVO})}$$
$$= \frac{B_{VVI}J_{VVI}R_{VVI}}{1+R_{VVO}/R_{VVI}} \ln\left(\frac{R_{VVO}}{R_{VVI}}\right),$$

where $J_{VVI} = I_2/(2\pi\Delta_{VV}R_{VVI})$ with Δ_{VV} being the VV thickness is the current density and $B_{VVI} \approx \mu_0(I_0 + I_1 + I_2/2)/(2\pi R_{VVI})$ the average magnetic field strength in the inboard VV wall.

The radial Lorentz force acting on the VV inboard wall is approximated by $-B_{VVI}J_{VVI}$ and we have

$$\sigma_\theta \approx -(B_{VVI}J_{VVI}\Delta_{VV})R_{VVI}/\Delta_{VV}$$
$$= -B_{VVI}J_{VVI}R_{VVI}.$$

using the cylindrical thin shell model.

We thus obtain the Tresca stress as

$$\sigma_{VV} = |\sigma_\theta - \sigma_Z| = \zeta B_{VVI}J_{VVI}R_{VVI},$$

where $\zeta = 1+(A_{VV}-1)\ln[(A_{VV}+1)/(A_{VV}-1)]/(2A_{VV})$ with the VV aspect ratio $A_{VV} = (R_{VVO}+R_{VVI})/(R_{VVO}-R_{VVI})$.

[1] ITER Design Description Document, DDD 11, Magnets, 8. Faults and Safety Assessment, ITER_D_ 22HVG6 v1.4 (2009).

[2] ITER Design Description Document, DDD 11, Magnet, 8. Fault and Safety Analysis, Annex 6a, “Assessment of the TF coil Circuit Behavior during Normal and Fault Conditions”, Bareyt, B; N 41 RI 34 00-11-01 W 0.1 (2009).

[3] Y. Itoh, H. Utoh, Y. Sakamoto and R. Hiwatari, “A Fast Discharge Scheme of Toroidal Field Coils for Fusion Demo Reactors”, Plasma Fusion Res. **14**, 1405167 (2019).

[4] K. Tobita *et al.*, “Japan’s Efforts to Develop the Concept of JA DEMO During the Past Decade”, Fusion Sci. Technol. 1943-7641 (2019).

[5] K. Yoshida, T. Isono, M. Sugimoto and K. Okuno, “Analysis program for Magnetic field, Inductance of Air-core Coils: COIL”, JAERI-Data/Code 2003-014 (2003).

[6] https://www.ansys.com/

[7] https://www.qst.go.jp/site/archives/1105.html

[8] ITER Design Description Document, DDD 11, Magnets, 2. TF coils and Structures, ITER_D_ 2MVZNX v2.2 (2009).

[9] H. Utoh *et al.*, “Design Study of Superconducting Magnets Based on Electromagnetic Field and Mechanical Analysis on JA DEMO”, in Japanese, Proc. JSPF Annual Meeting, 6Da04 (2018).

[10] S. Moriguchi, K. Udagawa and S. Hitomatsu, *Mathematical Formulas I*, in Japanese, Chap. 2, Sec. 26, p.120, (Iwanami, 1956).